



Composition of prehistoric rock-painting pigments from Egypt (Gilf Kébir area)

L. Darchuk^{a,*}, G. Gatto Rotondo^a, M. Swaenen^b, A. Worobiec^a, Z. Tsybrii^c,
Y. Makarovska^a, R. Van Grieken^a

^a Department of Chemistry, University of Antwerp, Universiteitsplein 1, 2610 Wilrijk, Antwerp, Belgium

^b Academy for Mineralogy, Frans de l'Arbreleaan 12, 2170 Merksem, Antwerp, Belgium

^c Department of IR Devices, Institute of Semiconductor Physics, NASU, pr. Nauki 43, Kyiv, Ukraine

ARTICLE INFO

Article history:

Received 27 April 2011

Accepted 20 June 2011

Keywords:

Rock-painting pigments

Red and yellow ochre

Micro-Raman

FTIR

SEM/EDX

XRF

ABSTRACT

The composition of rock-painting pigments from Egypt (Gilf Kebia area) has been analyzed by means of molecular spectroscopy such as Fourier transform infrared and micro-Raman spectroscopy and scanning electron microscopy coupled to an energy dispersive X-ray spectrometer and X-ray fluorescence analysis. Red and yellow pigments were recognized as red and yellow ochre with additional rutile.

© 2011 Elsevier B.V. All rights reserved.

1. Introduction

By default the prehistoric pigments were based on red and yellow natural earths (mainly yellow and red ochres), which have been universally used as pigments from the earliest history [1,2] and have been frequently found in many cave paintings. When we analyze pigments we very often run into mixtures of natural earths (ochre, sienna, and umber) and therefore their identification becomes more complex.

The majority of red pigments used in ancient Egypt was natural earth based on colours containing iron oxide. They have been applied on wood, on stone or in some other cultures even for skin-paintings [3–5].

Ochres are natural earths consisting of clayey minerals (kaolinite and illite) with impurities (gypsum, quartz, magnesium carbonate, and manganese oxide), and of various hydrated forms of iron oxide which give the colouration. Usually red colour is determined by presence of haematite (Fe_2O_3), while yellow colour is revealed when goethite ($\text{FeO}\cdot\text{OH}$) dominates.

Sienna is a natural variety of ochre whose colour has been stabilized by burning it at a high temperature to remove water from the clay and give a reddish-brown colour. The main ingredients of burned sienna are haematite (30–50%) and amorphous silica (10–30%) mixed with minor components of MnO_2 (0.1–1%), alu-

mina, quartz and calcium carbonate. Umber is a combination of iron oxide, manganese oxide and clays [2].

The goal of this work is the identification of pigments used for prehistorical rock-paintings. Samples of pigments were collected from two places in Egypt, the “New cave” situated in the west part of the Gilf Kébir area near the border of Libya (between Foggini cave and Wadi Sura), and “Water mountain”, located 100 km west of the oasis Dahkla. Prehistorical rock-paintings of probably around 8000 years old have been discovered on the ceiling and on the wall of the “Water Mountain”.

Located far away from the habited civilized places, the south western desert area of Egypt is famous for its ancient rock art such as paintings and engravings. Most of them come from people living there between 10,000 and 6000 years ago before the climate turned this area into a desert. The most known ones are the thousands of paintings found in the Uweinat area close to the border of Sudan and Libya. This area is one of the most remote places in the world with harsh climate, without any water sources and nearly 500 km far away from the next human being. Ancient Egyptian wall pigments from the pharaone's tombs have been analyzed extensively by X-ray fluorescence (XRF) and Raman spectroscopy [6–11], but only a few attempts have been made to characterize rock-painting pigments composition.

To get information about the composition of prehistorical rock pigments elemental analysis with scanning electron microscopy (SEM–EDX) and X-ray fluorescence has been performed. The obtained set of chemical elements could produce different compounds. So in order to identify such a compounds making up the prehistorical rock-paintings pigments, molecular spectroscopy

* Corresponding author. Tel.: +30 32 32652345.

E-mail address: larysa.darchuk@ua.ac.be (L. Darchuk).

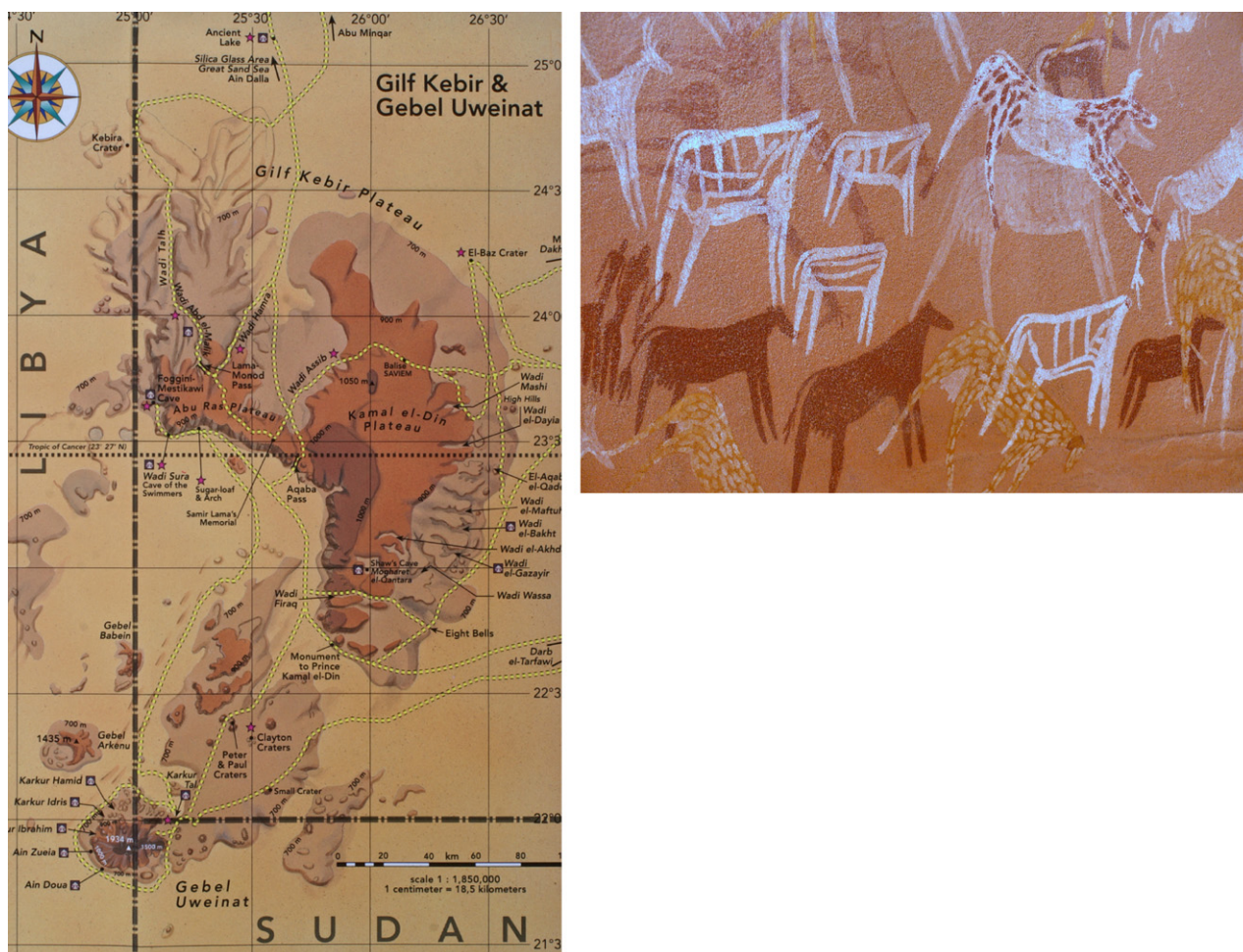


Fig. 1. Location of the site Gilf Kébir and rock painting on a ceiling of the “New cave”.

(micro-Raman spectroscopy (MRS) and infrared spectroscopy (FTIR)) was applied. The selection rules for Raman scattering are different from those for infrared absorption. Bands characteristic of a bond can be present in Raman scattering, in IR absorption or both. Combination of Raman and IR analysis has been used in order to get complementary information.

2. Experimentation

2.1. Samples

Five rock-painting pigment samples from “New cave” (samples **1**, **2**, and **3**) and “Water mountain” (samples **4** and **5**) were analyzed. The location of the site and the rock-painting on the ceiling of the “New cave” are shown in Fig. 1(a and b). The pigment powders of reddish and yellowish shades were scraped from different colour spots near the rock pictures and were stored into test-tubes.

2.2. Elemental analysis

2.2.1. Scanning electron microscopy analysis

In order to obtain the elemental composition of the pigments, a SEM/EDX was used.

An accelerating voltage of 20 kV and a current of 1 nA were applied during the measurements. The instrument was a JEOL 6300 SEM with a PGT EDX detector and super thin atmospheric window.

A small amount of the pigment grains was spread on the carbon double stuck tape. During the investigation only grains with minimum diameter of $4\ \mu\text{m}$ and maximum diameter of $10\ \mu\text{m}$ were analyzed. Geometrical diameter of the pigment grains was determined from the backscattered electron image.

Determination of the characteristic peak intensities was obtained by using the top-hat filter method [12].

The results were subjected to multivariate analysis to reduce the amount of data and to extract the relevant (pertinent) information. The same procedure as described by Darchuk et al. [13] was used.

2.2.2. X-ray fluorescence analysis

Bulk elemental analysis of the pigments was carried out with energy-dispersive X-ray fluorescence (XRF) spectrometer Epsilon 5 (PANalytical, Almelo, The Netherlands). The spectrometer equipped with 600 W tube with Gd-anode, 3D polarizing geometry with 15 secondary targets. Ti secondary target (40 kV, 15 mA) was used for excitation of Al K_{α} , Si K_{α} , S K_{α} , Cl K_{α} , K K_{α} lines for 5000 s. Ge secondary target (75 kV, 8 mA) was used for excitation of Ca K_{α} , Ti K_{α} , V K_{α} , Cr K_{α} , Fe K_{α} , Zn K_{α} lines for 1000 s.

For calibration of XRF spectrometer five standards have been used, as shown in Table 1. They were prepared by weighting the powders on an analytical balance with precision of 0.05 mg. Content of manganese oxide has been calculated by extrapolation based on a curve of sensitivity of the spectrometer. The pigment powders or a standard powders were placed between two Mylar films and analyzed with He system option.

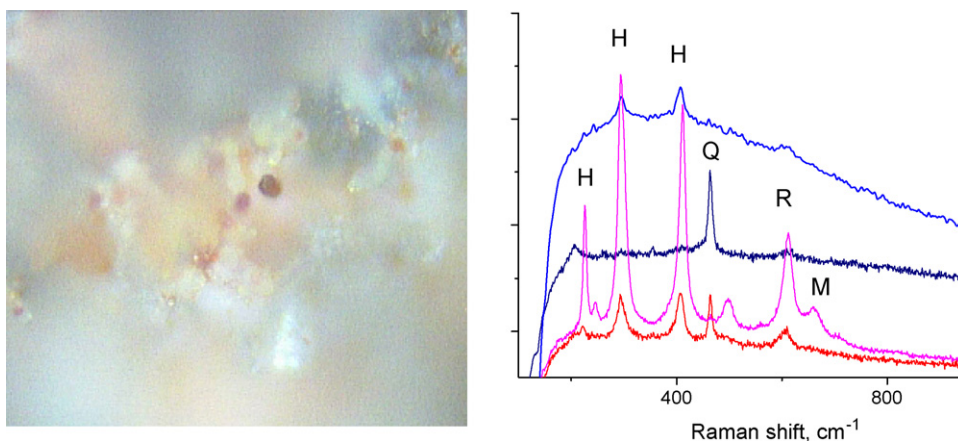


Fig. 2. Picture of the pigment from “New cave” (sample 1) and Raman spectra obtained from different areas of the pigment, H – haematite, Q – quartz, R – rutile, M – magnetite.

2.3. Molecular spectroscopy analysis

2.3.1. Micro-Raman spectroscopy

MRS measurements were carried out with a Renishaw InVia micro-Raman spectrometer (Renishaw, Wotton-under-Edge, UK) coupled with a Peltier cooled CCD detector. Argon lasers (514.5 nm) as well as a diode laser (785 nm) were applied for vibrational excitation. The green laser can sometimes damage the pigment grains, due to the sensitivity of iron-rich particles to the intensity and the wavelength of the laser beam [14], so low laser beam power has been applied to prevent burning of the pigment grains.

A spectral range between 100 and 3200 cm^{-1} with a spectral resolution of 2 cm^{-1} was used. Data acquisition was carried out with the Wire™ and Spectralcalc software packages from Renishaw (Wotton-under-Edge, UK) and GRAMS (Galactic Industries, Salem, NH, USA), respectively. Spectral analyses were performed by comparing the measured spectra with the ones from both an in-house library and a commercially available spectral library.

Grains of pigment powder were put on an aluminium foil used as substrate and they were analyzed manually.

The number of accumulations for each spectrum varied from 1 to 5 and they were added, in order to provide a better signal-to-noise ratio.

With a 100 \times magnification objective lens, spectra from grains from 1 μm size can be collected. For each investigated sample we collected at least 10 Raman spectra from different grains of the specimens to check the homogeneity of the pigments.

2.3.2. Fourier transform infrared spectroscopy

Infrared spectral analysis of the pigments was performed by a one-beam FTIR spectrometer Spectrum BX-II (Perkin Elmer, Wellesley, MA).

Table 1
Standards used for calibration of XRF spectrometer.

	Standard 1	Standard 2	Standard 3	Standard 4	Standard 5
Al (%)	3.62	4.12	5.26	3.98	4.16
Si (%)	12.588	20.019	23.588	29.927	16.173
S (%)	0.018	0.017	0.026	0.020	0.585
Cl (ppm)	287	380	192	105	656
K (%)	0.113	0.020	0.151	0.093	0.716
Ca (%)	0.191	0.099	0.230	0.226	0.531
Ti (%)	0.137	0.883	0.976	1,331	0.320
V (ppm)	3940	18,066	28,339	45,894	6271
Cr (ppm)	34	38	99	149	87
Fe (%)	0.544	1.648	4.027	8.724	0.791
Zn (ppm)	183	439	749	804	606

Table 2
Elemental composition analysis results.

Elements	Sample 1	Sample 2	Sample 3	Sample 4	Sample 5
Al (%)	3.04	2.89	2.07	2.73	2.57
Si (%)	28.1	33.8	31.0	18.5	29.0
S (%)	0.0068	0.0071	0.0036	0.0053	0.2069
Cl (ppm)	75	67	46	74	120
K (%)	0.037	0.162	0.079	0.127	0.739
Ca (%)	0.033	0.068	0.046	0.096	0.196
Ti (%)	0.60	0.507	0.448	0.092	0.245
V (ppm)	101	281	310	43	38
Cr (ppm)	15	18	16	4	15
Fe (%)	1.45	3.17	3.48	0.51	0.89
Zn (ppm)	152	184	128	57	187
Mn (ppm)	32	54	46	32	20

A thin layer of the pigment powder was deposited on a KBr slice; no other sample preparation was required.

Transmission spectra of the pigments were obtained in the spectral region 400–4000 cm^{-1} with a spectral resolution of 2 cm^{-1} . An acquisition time of 60 s for each scan has been applied. It was determined that 5 co-averaged scans were enough to produce spectra of the desired quality, without any need to increase more the number of scans. FTIR spectra have been collected from several spots of the specimens. Diameter of analyzed spot depends on diaphragm applied, which was around 1 mm.

Literature data were used for the identification of the analyzed pigments.

3. Results and discussion

Tables 2 and 3 present elemental composition analysis and clustering analysis results obtained from the applied micro analytical techniques.

Table 3
Clustering analysis results exhibit percentage of clusters for each sample.

Clusters (%)	Sample 1	Sample 2	Sample 3	Sample 4	Sample 5
Clays	16.5	–	11.0	7.5	–
Clays + Fe oxides	40.0	21.5	28.0	50.0	10.0
Quartz	–	12.0	6.0	5.0	13.0
Fe-oxides	15.0	14.5	15.0	4.5	20.0
Fe-oxides + Al-Si	20.0	27.5	24.5	22.5	24.5
Clays + gypsum	3.0	1.5	–	–	–
Ti + Fe-oxides (+AlSi)	3.5	1.5	2.5	1.0	4.0
Al-oxides	–	–	1.5	–	–
Quartz + Fe-oxides	–	21.5	4.5	–	–
Calcite + Fe-oxides	–	–	7.0	9.0	28.0
Others	2.0	–	–	0.5	0.5

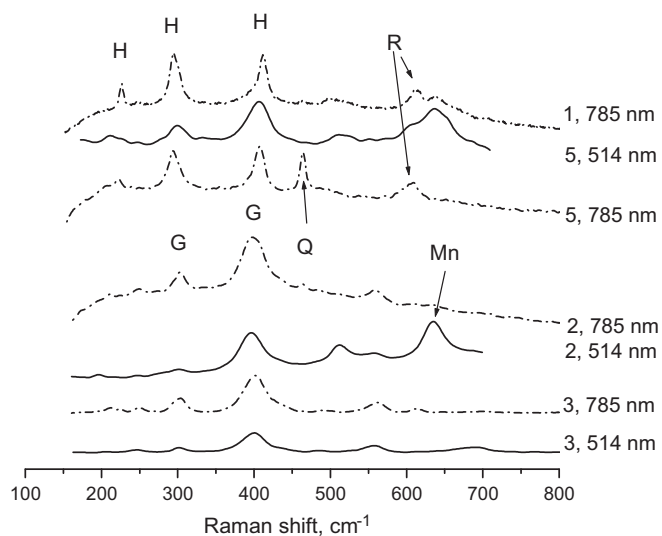


Fig. 3. Raman spectra of the analyzed pigments.

Both the clustering analysis and micro-Raman spectroscopy show inhomogeneous structure of all pigments typical of natural earth. From the clustering analysis of the pigments it is possible to distinguish set of clusters mainly based on clays and iron oxides (Table 3). According to Raman spectra the analyzed pigments consist of grains rich in iron oxide, quartz and aluminosilicate (Figs. 2 and 3).

3.1. Sample 1

Elemental composition analysis showed that violet-reddish sample 1 consists of 28.1% of Si, 1.45% of Fe, and the highest, compared to the other analyzed pigments amount of Al (3.04%) and Ti (0.60%) (Table 2). Agglomerations of clays based on aluminosilicates with iron oxide are principal clusters for the pigment (Table 3). About 15% of clusters are referred to iron oxides. Sample 1 consists of the biggest amount of clusters rich in both titanium and iron oxides (3.5%). Agglomerates of clays and gypsum formed around 3% of it.

Molecular spectroscopy analysis helped to distinguish between different forms of iron oxides, such as haematite, goethite or magnetite. The characteristic Raman bands of haematite (Fe_2O_3) at 225, 290–294, and 408 cm^{-1} have been identified in the spectra of sample 1 (Figs. 2b and 3). Also titanium presence as rutile (TiO_2) with typical bands at 445 and 610 cm^{-1} was found. Bands typical of quartz (SiO_2) at 252 and 465 cm^{-1} and of manganese oxide (MnO_2) at 640 cm^{-1} have been observed in some analyzed spots.

FTIR spectra of the samples 1 confirmed the presence of haematite recognized by the characteristic absorption bands of iron oxide (470 and 535 cm^{-1}) and the absence of the peak at 3140 cm^{-1} attributed to OH-group (Fig. 4). Absorbance peaks attributed to aluminosilicate at 1032 and 1009 cm^{-1} , as well as quartz at 684, 778, 798, 1085, and 1166 cm^{-1} [15] have also been detected.

3.2. Sample 2

According to elemental analysis 2.89% of Al, the highest amount of Si (33.8%), 0.507% of Ti, and high amount of Fe (3.17%) are the main components of yellow gold sample 2 (Table 2). Clusters rich in clays and gypsum have been detected for sample 2 as well for sample 1 (Table 3). Around 12% of clusters are comprised by quartz. High amount (about 22%) of agglomerates consisted of quartz and iron oxide is feature of sample 2.

Raman spectra of the sample showed presence of vibration bands typical of goethite (at 250 and 395 cm^{-1}), as shown in Fig. 3. The band at 640 cm^{-1} of MnO_2 was detected in the Raman spectra as well as for sample 1.

The FTIR spectra also consist of characteristic absorption bands of goethite: the bands at 470, 535 cm^{-1} arose from iron oxide and the band at 3140 cm^{-1} assigned hydroxyl stretch [16]. The presence of aluminosilicate produces an infrared spectrum with bands at 1032 and 1009 cm^{-1} . The bands at 684, 778, 798, 1085, and 1166 cm^{-1} were attributed to quartz (Fig. 4).

3.3. Sample 3

Elemental composition of the dark-yellow (sample 3) rock-painting pigment from the “New cave” showed that Si (31%), Al (2.07% the lowest amount), highest amount of Fe (3.48%) and of Ti (0.448%) as the principal elements (Table 2). Clusters formed by Al oxide (1.5%) are a particularity of sample 3. Presence of two types of clusters – iron oxides and quartz (4.5%) along with iron oxides with calcite (7%) was detected only for this sample (Table 3).

Raman bands corresponded to goethite (at 250 and 395 cm^{-1}), quartz (at 465 cm^{-1}) and rutile (at 445 and 610 cm^{-1}) as well as for gold-yellow pigment 2 (Fig. 3). Raman spectra of sample 3 lack the band at 640 cm^{-1} typical of manganese oxide, which differ them from those for sample 2.

The FTIR spectra of sample 3 consist of bands assigned to goethite, aluminosilicate and quartz and look like those of yellowish sample 2 (Fig. 4).

3.4. Sample 4

Orange-red sample 4 consists of 2.73% of Al, and the lowest amount of Si (18.5%), Fe (0.51%), and Ti (0.092%). Amount of clusters based on iron oxides is small (4.50%), iron oxides mainly exhibit as agglomerates with clays (50%) and aluminosilicate (22.5%). Agglomerates of iron oxides with calcite (9%) were detected as well. Only a few clusters consist of Ti along with Fe oxides.

Raman spectra for sample 4 were not informative and mainly showed huge fluorescence background caused by clay. For some

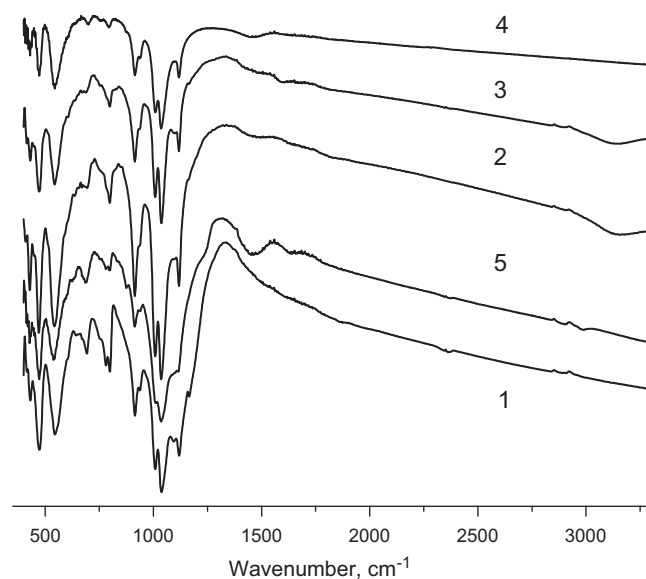


Fig. 4. Transmission IR spectra of the analyzed prehistoric pigments: the peak at 3140 cm^{-1} is attributed to OH-group, the absorption bands at 470 and 535 cm^{-1} belong to iron oxide, the bands at 684, 778, 798, 1085 and 1166 cm^{-1} are attributed for quartz, and bands of kaolinite were detected at 1032 and 1009 cm^{-1} .

pigment grains weak band corresponding to quartz (at 465 cm^{-1}) appeared.

Information about molecular composition of the pigment was got with FTIR spectroscopy. Presence of haematite has been recognized by the characteristic absorption bands of iron oxide (470 and 535 cm^{-1}) and absence of the peak at 3140 cm^{-1} attributed to OH-group (Fig. 4).

3.5. Sample 5

According to the elemental analysis, 29.0% of Si, 2.57% of Al, and low amount of Fe (0.89%) are the main components of the brown-red sample 5 from the “Water mountain”. Presence of clusters formed by iron oxides and calcite looks similar as for samples 3 and 4, but for sample 5 the biggest amount (28%) of iron oxides with calcite agglomerates was detected (Table 3). Like for all analyzed pigments agglomerates of both Ti and Fe oxides (4%) have been shown. The biggest amount of clusters based on iron oxides (20%) is a particularity of sample 5.

With micro-Raman spectroscopy iron oxide composed sample 5 was recognized like haematite and magnetite. The Raman spectra (Fig. 3) showed vibration bands typical of haematite and quartz. Using the laser with excitation at 514 cm^{-1} it is possible to see the wide band at 650 cm^{-1} which is overlapping of the bands typical of manganese oxide (at 640 cm^{-1}) and magnetite (at 665 cm^{-1}).

FTIR analysis of the pigments confirmed the Raman results. The presence of haematite, aluminosilicate and quartz was revealed in infrared spectra by their typical absorption bands. The aluminosilicate was identified by the Si–O–Si band at 1032 cm^{-1} , the Si–O–Al band at 1009 cm^{-1} and the Al–O–H band at 916 cm^{-1} . The bands at 684 , 778 , 798 , 1085 , and 1166 cm^{-1} were attributed to quartz.

4. Conclusions

Thanks to their complementarity, the applied techniques permitted to analyze and identify the prehistorical rock painting pigments from Egypt.

The basic components of the investigated prehistoric pigments are yellow or red ochre consisting of iron oxides, which give yellow,

red, and brown colours. The elements determined as major components are Al, Si, Ti and Fe, with small amount of Ca and traces of Mn.

The prehistorical pigments contain high percentage contributions of Si-rich (quartz, SiO_2) and Al–Si-rich particle types, most likely as a form of aluminosilicate $(\text{Al}_2\text{Si}_2)_5(\text{OH})_4$ and montmorillonite $((\text{Na,Ca})_{0.3}(\text{Al,Mg})_2\text{Si}_4\text{O}_{10}(\text{OH})_2 \cdot n(\text{H}_2\text{O}))$. Iron oxides (haematite or goethite) and titanium oxide have been detected as incorporation into grains of aluminosilicates (Al–Si–Fe rich particle types).

Acknowledgement

The support from the FWO (Fund for Scientific Research – Flanders, Belgium) for post-doctoral researcher Anna Worobiec is appreciated.

References

- [1] T.A. Wertime, J.D. Muhyl, *The Coming of the Age of Iron*, Yale University Press, New Haven, 1980.
- [2] R.J. Gettens, G.L. Stout, *Paintings Materials – A Short Encyclopedia*, Dover Publ., Inc., New York, 1966.
- [3] W.V. Davies, *Colour and Painting in Ancient Egypt*, Oxbow Books, London, 2001.
- [4] M. Uda, S. Sassa, S. Yoshimura, J. Kondo, M. Nakamura, Y. Ban, H. Adachi, *Instrum. Nucl. Methods B* 161–163 (2000) 758.
- [5] G.M. Edwards, E. Villar, A. David, L.A. de Faria, *Anal. Chim. Acta* 503 (2004) 223.
- [6] J. Ambers, *J. Raman Spectrosc.* 35 (2004) 768.
- [7] A.R. David, H.G.M. Edwards, D.W. Farwell, D.L.A. De Faria, *Archaeometry* 43 (2001) 461.
- [8] L. Burgio, R.J.H. Clark, *J. Raman Spectrosc.* 31 (2000) 395.
- [9] P. Vandenaabeele, A. von Bohlen, L. Moens, R. Klockenkamper, F. Joukes, G. Dewispelaere, *Anal. Lett.* 33 (2000) 3315.
- [10] G.M. Edwards, E. Villar, A. Eremin, *J. Raman Spectrosc.* 35 (2004) 786.
- [11] S. Colinart, M. Menu, *La Couleur dans la Peinture et l'Émailage de l'Égypte Ancienne*, Edipuglia, Bari, 1998.
- [12] R. Van Grieken, A.A. Markowicz, *Handbook of X-Ray Spectrometry*, Marcel Dekker, New York, 1993.
- [13] L. Darchuk, Z. Tzybrii, A. Worobiec, C. Vázquez, O.M. Palacios, E.A. Stefaniak, G. Gatto, F. Sizov, R. Van Grieken, *J. Spectrochim. Acta A* 75 (2010) 1398.
- [14] A. Worobiec, L. Darchuk, A. Brooker, H. Potgieter, R. Van Grieken, *J. Raman Spectrosc.* 42 (2011) 808.
- [15] D. Bikiaris, S. Daniilia, S. Sotiropoulou, O. Katsimbiri, E. Pavlidou, A. Moutsatsou, Y. Chrysoulakis, *Spectrochim. Acta A* 56 (2000) 3.
- [16] C. Genestar, C. Pons, *Anal. Bioanal. Chem.* 382 (2005) 269.